A&A manuscript no.

AA2343E

Your thesaurus codes are:
07(08.09.2 BF Aur; 08.02.2; 08.05.1; 08.02.1; 08.05.3)

ASTRONOMY AND ASTROPHYSICS

June 2, 2000

The BF Aurigae system⋆

A close binary at the onset of mass transfer

J. Kallrath[1] **and K.G. Strassmeier**[2,⋆⋆]

[1] BASF-AG, ZDP/C-C13, 67056 Ludwigshafen, Germany (josef.kallrath@basf-ag.de)
[2] Institut für Astronomie, Universität Wien, Türkenschanzstrasse 17, 1180 Wien, Austria (strassmeier@astro.univie.ac.at)

Received 28 January 2000 / Accepted 28 April 2000

Abstract. Because the question of the mass ratio of the early-type system BF Aur has not yet fully been clarified, we present and analyse new UBV photometry and nearly contemporaneous radial velocity observations. From a simultaneous least squares analysis of the photometric light curves and the new radial velocity curves we derive a mass ratio of $q = 1.048 \pm 0.02$. With even much more accurate photometric and spectroscopic data the mass ratio remains weakly defined. The resulting stellar parameters are consistent with line ratios derived from old and our new spectra and available Strömgren indices. We confirm earlier conclusions that BF Aur is detached and that the more massive component is almost filling its Roche lobe. New data indicating a period change support the interpretation that mass exchange has already started or is about to start.

Key words: stars: individual: BF Aur – stars: binaries: eclipsing – stars: early-type – stars: binaries: close – stars: evolution

1. Introduction: the BF Aurigae system

BF Aur (=HD 32419=BD+41°1051; α_{1950}=05$^{\rm h}$01$^{\rm m}$33.0, δ_{1950}=+41°13′13″, P=1$^{\rm d}$.5832179) was discovered as an eclipsing binary by Morgenroth (1935) and has a long history in eclipsing binary research briefly summarized by Kallrath & Kämper (1992; KK hereafter). The spectral classification, B5V (Roman 1956) and confirmed by Popper (1980), was found roughly consistent with normal main-sequence components of about $5\mathcal{M}_\odot$.

KK's analysis used UBV data by Mannino et al. (1964), as well as Strömgren indices and the line ratio. It puts some bounds on the mass ratio which they determine as $q = 1.05 \pm 0.05$. Their analysis shows some preference for a solution in which the stars almost fill their Roche lobes.

Van Hamme's (1993b) analysis based on the Mannino et al. (1964) photometric data and the radial velocities by Mammano et al. (1974) shows that multiple reflection does not play an important role. According to his least squares fits obtained with the 1993 version of the Wilson-Devinney (WD) model, BF Aur appears to be detached with very similar components filling approximately 95% to 97% of their Roche lobes.

Demircan et al. (1997) used new UBV photometry that they obtained during 19 nights in August 1988 and March 1989 and the Mammano et al. (1974) radial velocity curves in a simultaneous least-squares analysis. However, they could not overcome the ambiguity in the photometric data and ask for more accurate radial velocity data before claiming uniqueness.

We analyze new, much more accurate, photometric and spectroscopic data simultaneously and try again to decide whether BF Aur is detached or semi-detached and whether the primary minimum is a transit or an occultation. We aim to give a precise mass ratio and the absolute parameters of the system and discuss the evolutionary status of BF Aur in the light of the available spectroscopic and photometric evidence, including the period change obtained by Demircan et al. (1997).

2. Observations

2.1. Spectra and radial velocities

Eighteen spectroscopic observations were obtained with the 0.9-m coudé feed telescope at Kitt Peak National Observatory (KPNO) during Mar. 31 – April 21, 1998. We used the Ford F3KB CCD with grating A, camera 5, the blue corrector, and the long collimator. The spectra cover the wavelength region between 424 and 454 nm. The resolving power, $\lambda/\Delta\lambda$, was 22,000 corresponding to an effective wavelength resolution of 0.20 Å. The instrumental FWHM was sampled by 2.8 pixels according to a slit width of 400 μm. All spectra were obtained with an integration time of 30 min and have S/N ratios in the continuum between (60–100):1. Data reduction was performed with IRAF and consisted of bias subtraction, flat fielding, and optimized aperture extraction. A representative spectrum near quadrature is shown in Fig. 1.

Spectra of the radial-velocity standard β Gem (K0III) and the B5V reference star α Leo were obtained at least once dur-

Send offprint requests to: K.G. Strassmeier

⋆ Tables A1–A5 are available electronically only at the CDS via anonymous ftp (130.79.128.5) ftp://cdsarc.u-strasbg.fr or http://cdsweb.u-strasbg.fr/index.htm

⋆⋆ Visiting Astronomer, Kitt Peak National Observatory, operated by the Association of Universities for Research in Astronomy, Inc. under contract with the National Science Foundation

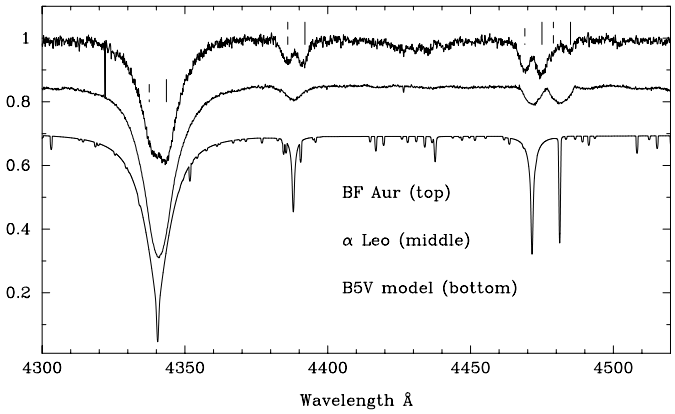

Fig. 1. A representative spectrum of BF Aurigae (top). The markers indicate the primary (full lines) and the secondary (dashed lines). As a comparison, we also show a spectrum of the single star α Leo (B5V) and a synthetic spectrum from a 15,000 K and $\log g$=4 model atmosphere. The strong line at 4340 Å is Hγ.

ing each night to enable an accurate wavelength calibration. However, fitting two Gaussians for the two components to the nightly cross-correlation functions, obtained with IRAF's `fxcor` task, did not result in the desired small residuals for an individual radial-velocity measurement because, firstly, β Gem is of significantly different spectral type compared to BF Aur and, secondly, the spectral lines of α Leo are too broad to result in a sharp cross-correlation peak. Therefore, we computed a theoretical spectrum from a 15,000 K and $\log g$=4.0 ATLAS-9 model atmosphere and used this spectrum as a reference spectrum (Fig. 1). The heliocentric radial velocities of the individual stellar components were then obtained by a least-squares fit of a combination of two of these theoretical spectra, appropriately rotationally broadened, wavelength shifted, and intensity weighted to match the BF Aur spectra. The resulting velocities are given in Table 1 (in column $v_{\rm helio}$) and are based on the wavelength shifts of the following spectral features: Balmer Hγ, He II 438.7 nm, He I 447.1 nm, and Mg II 448.1 nm. This procedure does not allow to compute a formal error because the overall χ^2 also depends on the match of the line intensities rather than solely on wavelength position. We estimate the internal precision of a single measurement to ± 5 km s^{-1} at quadrature and to $\pm$10–15 km s^{-1} near conjunction based on a comparison with other data taken during the same nights.

2.2. Photometry

Johnson UBV photometry was obtained with one of the two 0.75-m Vienna Observatory automatic photoelectric telescopes in southern Arizona (for details see Strassmeier et al. 1997) in the time between January and March 1998 just prior to the spectroscopic observations.

Altogether, 387 U-, 342 B-, and 320 V- points are presented in Tables A1–A5 (only in electronic form). The integration time was 60 s per reading and the observations were arranged in the sequence C2 – S – C1 – V – C1 – S – C2, where V denotes the measurement on BF Aur, C1 refers to the comparison star, HD 32330 (B2IV), C2 to the check star, HD 32418 (A4V), and S to sky measurements. This sequence was carried out repeatedly for U, B, and V, and took 7 minutes per filter including recentering the star after each filter sequence. For the reduction procedure, we use the average <V–C1> count rates of each sequence. The standard error of a single C2–C1 mean from the overall mean was $0\overset{\rm m}{.}0025$ in BV and $0\overset{\rm m}{.}003$ in U.

Table 1. Radial velocities in km s^{-1} (P = primary, S = secondary). The last two columns, $v_{\rm helio}$, denote the heliocentric radial velocities of the primary and secondary. Phase has been computed with the ephemeris given in Demircan et al. (1997).

HJD	Phase	$v_{\rm rel}$		Hel.	$v_{\rm helio}$	
(2450+)		P	S	corr.	P	S
904.6117	0.7156	-170	212	-26.59	-157.5	224.5
906.6193	0.9836	-2	44	-26.21	10.9	56.9
907.6305	0.6223	-113	162	-26.03	-100.0	175.1
908.6098	0.2409	214	-168	-25.80	227.3	-154.7
909.6121	0.8740	-122	158	-25.59	-108.5	171.5
910.6092	0.5037	2	22	-25.36	15.7	35.7
911.6140	0.1384	157	-136	-25.14	170.9	-122.1
912.6083	0.7664	-177	221	-24.90	-162.8	235.2
913.6079	0.3978	143	-95	-24.65	157.4	-80.6
914.6081	0.0295	87	-24	-24.41	101.7	-9.3
916.6080	0.2927	213	-167	-23.89	228.2	-151.8
917.6083	0.9245	-75	124	-23.62	-59.5	139.5
918.6078	0.5558	-77	74	-23.35	-61.3	89.7
920.6104	0.8207	-148	207	-22.78	-131.7	223.3
921.6114	0.4530	105	-50	-22.49	121.6	-33.4
922.6110	0.0843	123	-93	-22.19	139.9	-76.1
923.6095	0.7150	-181	206	-21.88	-163.8	223.2
925.6135	0.9808	-34	41	-21.25	-16.2	58.8

3. Simultaneous photometric and spectroscopic least-squares solution

In agreement with the line-ratio discussion in Sect. 4.1 and the discussion of nomenclature in Kallrath & Milone (1999, Sect. 2.7), we refer to the primary component labelled by index 1 as the photometric primary (the star eclipsed at primary minimum). The photometric primary corresponds to the spectroscopic secondary star (the star with the weaker spectral lines). The spectroscopic primary is eclipsed at secondary minimum.

To solve the light curves, we used the software package `WD98`, a successor of `WD95` (Kallrath et al. 1998) based on the 1993 version of the WD code, and a further improved version, called `WD98`, based on the 1998 version of the WD code. The least-squares problem of parameter estimation is treated in the usual way described in Kallrath & Milone (1999, Chapter 4).

We used all observations described in Sect. 2, *i.e.*, 18 individual data points in the radial velocity curve, 387, 342, and 320 in *U*, *B*, and *V* with the Levenberg-Marquardt scheme. The individual weights w_i are computed as

$$w = w^{\rm flux} w^{\rm c}, \qquad (1)$$

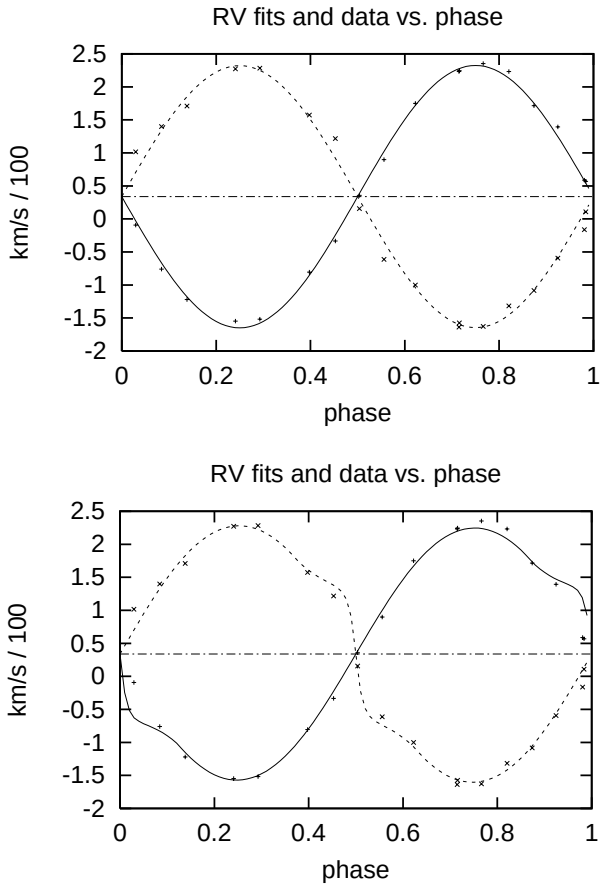

Fig. 2. Radial velocity curves (solid line is star 1, dashed line is star 2) and fits obtained when proximity effects are excluded (top panel) and included (bottom panel). The fit is improved significantly when proximity effects are included. The standard deviation of the fits decreased from 11.693 to 10.008 km s^{-1} as shown in Table 2. We estimate the internal precision of a single measurement to ± 5 km s^{-1} at quadrature and to ± 10–15 km s^{-1} near conjunction based on a comparison with other data taken during the same nights.

with the following meaning:

- $w^{\rm flux}$ is a flux-dependent weight chosen proportional to the phase-dependent inverse flux $1/l$ of the binary system [for details, see Kallrath & Milone (1999, p.103], as appropriate for photon statistics ($b = 1/2$ in the nomenclature of Linnell & Proctor 1970); and
- $w^{\rm c}$ is a curve-dependent weight accounting for the standard deviation of the data points in that curve.

The factors $w^{\rm flux}$ and $w^{\rm c}$ are described in detail in Wilson (1979) and Kallrath & Milone (1999). Calculations were performed either in mode 2 (cf. Wilson 1988), *i.e.*, L_2 is coupled to T_2 through the Planck function, while no geometrical constraints are imposed, or in mode 5 (which forces the secondary component to fill its Roche lobe). In `WD98` all configurations possible in the Roche model (detached, semi-detached, contact, over-contact) may be realized within mode 2. That means, if one or both stars overfill their Roche lobe, the corresponding lobe-filling constraint is automatically applied. We fixed the temperature of the primary at $T_1 = 15800$ K estimated from its spectral type B5V (Popper 1980).

Table 2. Parameters derived from the radial velocities. The fitted parameters are the semi-major axis, a, the systemic velocity, γ and the mass ratio, q.

Proximity effects	$\sigma_{\rm fit}$ [km s^{-1}]	a [R$_\odot$]	γ [km s^{-1}]	q [-]
excluded	11.693	12.474	33.770	1.0015
	11.693	$\pm$0.167	+ 19.491	$\pm$0.0275
included	10.008	12.276	33.783	0.9787
	10.008	$\pm$0.140	+ 16.869	$\pm$0.0214

The strong correlation of the limb-darkening coefficients with other light-curve parameters and its negative influence on the numerical properties of the light curve is a well-known problem (see, e.g., Wilson & Devinney 1971, or Twigg & Rafert 1980). Only under exceptional circumstances (i.e. total eclipses) will it be possible to extract meaningful limb-darkening coefficients. In view of these difficulties it is perhaps the wisest to trust the coefficients derived from the best available model atmospheres. Therefore, we adopted the square root and, alternatively, in some additional test runs the logarithmic limb-darkening coefficients given by Van Hamme (1993a), which are based on the model-atmosphere grid of Kurucz (1979). For BF Aur as an early type system the square-root coefficients, $x_{1,2}$ and $y_{1,2}$, seem to be more appropriate and we used

	U	B	V	bol
$x_{1,2}$	0.005	-0.084	-0.070	0.602
	0.005	-0.083	-0.070	0.602
$y_{1,2}$	0.583	0.736	0.623	0.172
	0.583	0.733	0.620	0.172.

Van Hamme's (1993a) interpolation software was used to derive these values. If the temperature of the secondary component changed in the course of the iterations, the limb-darkening coefficients were adopted accordingly.

The albedos were fixed at the values appropriate for radiative envelopes, $A_1 = A_2 = 1$, corresponding to full reradiation. Gravity darkening exponents $g_1 = g_2 = 1$ were chosen, corresponding to von Zeipel's law.

Since the new observations are of high quality and are consistent in time, a simultaneous analysis of both radial-velocity curves and the U, B and V curves seemed warranted. However, at first we analyzed the radial-velocity curves separately which gave a mass ratio q almost identical to unity. Fig. 2a shows the radial velocity curves and the fits when proximity effects were excluded from the model, i.e., only the semi-major axis, a, the system velocity, γ, and the mass ratio, q, were free parameters. Fig. 2b shows the fit when proximity effects are included. The results are quantified in Table 2.

The fit including proximity effects (turned on by the control flags `ICORR1` and `ICORR2` in the `WD` program set to 1) requires that the shapes of the stars and the surface flux distribution are known. This was achieved by adopting some of the parameters obtained in the simultaneous analysis. Note that the fit and its

standard deviation is better and that the standard deviations of the estimated parameters are smaller. Therefore, we continued to model the radial velocities with the proximity effects. Note that the uncertainty in the mass ratio ($q = 0.9787 \pm 0.0214$) prevents us from deciding whether q is smaller or larger than 1. A definite decision requires much more accurate radial velocity data than our 5 km s^{-1} rms. Unfortunately, as has already been shown by KK the photometric data (in the case of BF Aur) put no further constraints on q as long as $0.9 \leq q \leq 1.1$. This fact is consistent with the experience that the mass ratio q, although it may in principle be obtained for close binary systems from light curve synthesis, is often a quite weakly determined parameter, for near-contact binaries (see, e.g., the discussions in Breinhorst et al. 1989 or Kaluzny & Semeniuk 1984) and indeterminate for well-detached ones. A semi-detached solution constraint may often give a quite definitive photometric mass ratio, being based more on the size of the lobe filling star than its distortion; however, can we be sure that the system is really semi-detached?

Since q is so weakly defined, we used a grid approach (see Kallrath & Milone 1999, Appendix B, or KK) to trace the quality of the fit as a function of q. Table 3 gives a sequence of solutions obtained with the Levenberg-Marquardt scheme for fixed mass ratio. The solutions in this table have been produced by following a homotopy track, i.e., the solution for $q = 0.80$ served as the initial guess for $q = 0.81$ and so on. The table shows that q is probably very close to unity; and it is very difficult to decide whether we have mass reversal or not. Note that all solutions refer to detached solution as is indicated by $f_1 < 0$ and $f_2 < 0$. A similar run has been performed enforcing that the secondary component is lobe filling (mode 5 in Wilson's program). The results were slightly worse as shown in Table 4.

For completeness, we give in Table 7 those values which can be derived from the finally adopted solution (surfaces $S_{\rm k}$, volumes $V_{\rm k}$, mean radii $\bar{r}_{\rm k}$). Figs. 3 and 4 show the final solutions of the light curves and the radial velocity curves, respectively.

4. Consistency checks with other observational facts

We now check whether further observational facts that were not included in the simultaneous analysis, such as line ratios, Strömgren indices, and period change, are consistent with the model produced by the least-squares solution.

4.1. The spectral line ratio of He I *438.7 nm*

As the components have almost equal temperatures (with $T_1 > T_2$) and similar surface gravities the line-strength ratio should compare well with the luminosity ratio $\ell_{\rm SP}/\ell_{\rm SS}$. Popper (1981) reproduced microphotometer tracings of the spectra of 26 OB eclipsing binaries in the wavelength range 430–450 nm. The BF Aur spectrogram illustrated in his Fig. 7 corresponds to phase $0\overset{\rm p}{.}70$, i.e., the component eclipsed at primary minimum is receding. Lines of both stars are clearly present, the redshifted components all being the weaker ones. From $H\gamma$ and He I 438.7, Kallrath & Kämper (1992) estimated a line ratio of roughly 1.3 ± 0.1, in agreement with the statement made already by Mammano et al. (1974) (but ignored by later investigators) that the spectroscopic component 2 is the one being eclipsed at primary minimum, i.e., corresponds to the photometric primary. Thus, KK accepted only solutions with line ratios close to that value. Their B solutions (KK Tables 1 and 2) had a line ratio of about 1.2.

The line ratios of our new spectroscopic data were evaluated at four quadrature phases for the He I line at 438.7 nm, and lead to the line-depth ratio (primary/ secondary) of 1.24 ± 0.08 (rms) as measured from the residual intensities in the respective line cores. A double-Gaussian fit with the routines supplied by the NOAO/IRAF data-reduction package yields an equivalent-width ratio of 1.24 ± 0.12 (rms) in good agreement with above value. The individual equivalent widths for the star with the stronger lines are between 402–376 mÅ and for the star with the weaker lines between 360–290 mÅ. The average internal rms error from the two-Gaussian fits was 8 mÅ. Fig. 1 shows a representative spectrum near quadrature. Note that the line profiles are never completely blend free and the internal rms error is thus likely underestimated.

Let us now compare these observational facts with the computational results summarized in Table 8 which shows the ratio $\ell_{2B}(\theta)/\ell_{1B}(\theta)$ as a function of phase θ and the mass ratio q; these values were computed with Wilson's subroutine LC. The mass ratio $q = 0.961$ ($q = 1.048$) corresponds to the solution in Table 5 (6).
Compared to the observational values, the values in Table 8 slightly indicate a preference for the $q = 1.048$ solution, for which the computational light ratio are just within the error bounds of the observational line ratios. For the solution corresponding to $q = 0.961$ the computational values are slightly out of the error bounds of the observational values. In Table 3 we note that solutions for $q < 0.99$ have $\ell_B < 1.1$ and that these solutions are thus not consistent with the observed line ratios.

4.2. The influence of the reflection effect on the solution

The influence of the reflection effect, and in particular how significant multiple reflection is in the BF Aur system, has been analyzed by KK and by Van Hamme (1993b). For the solution in Table 3, we confirm again that multiple reflection is not significant in the BF Aur system, i.e., does not change the estimated parameters at all.

4.3. Additional information from Strömgren indices

Strömgren indices for BF Aur measured at five phases are available from the survey by Hilditch & Hill (1975). Because the components have almost equal temperature and similar surface gravities, their colors will be similar and we may take the indices measured as representative of either component, after correction for interstellar extinction. The indices measured can be dereddened with Crawford's (1978) intrinsic color relations for B-type stars. Taking the slope of the reddening line in the $(u - b)$ vs. $(b - y)$ diagram to be 1.5, one

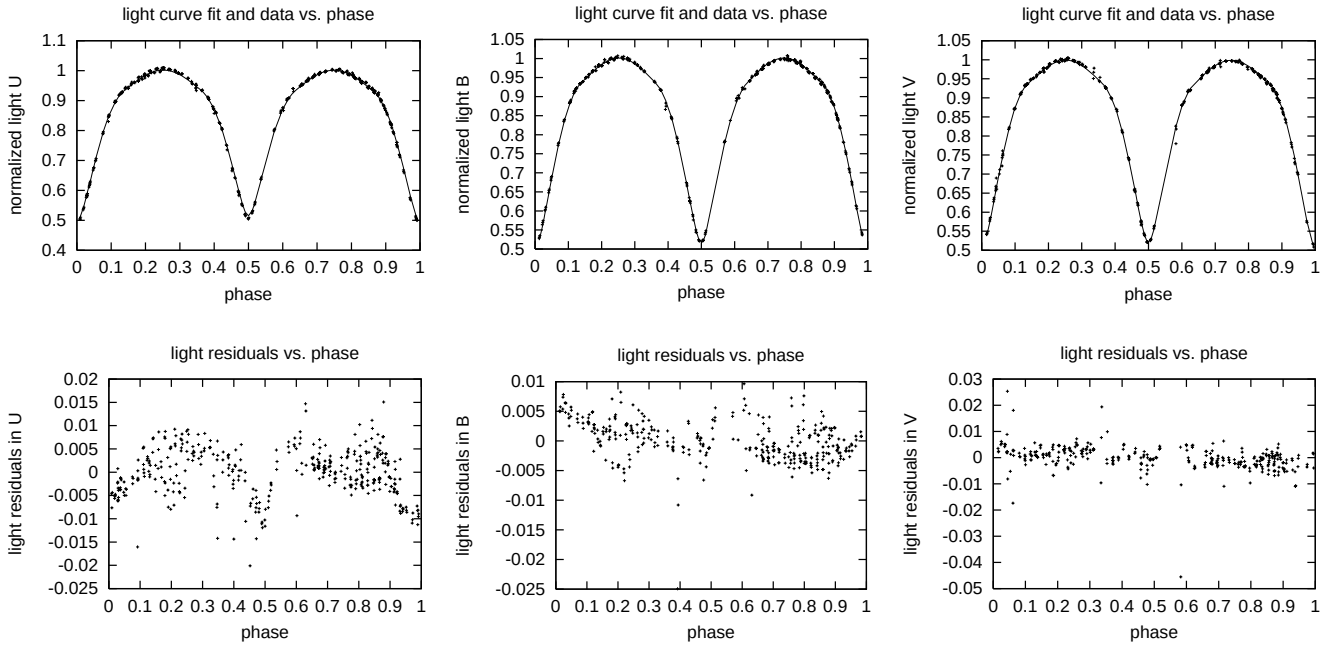

Fig. 3. Differential UBV light curves showing normalized flux in the specific passbands versus phase, and their respective fits. The lower panels show the residuals.

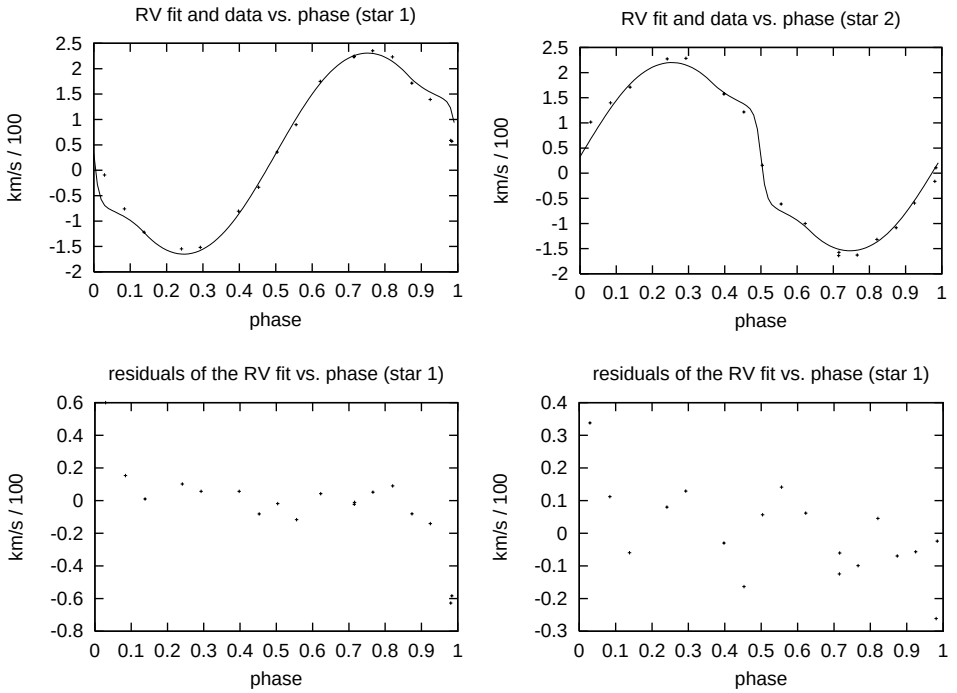

Fig. 4. Radial-velocity fits from the simultaneous solution (Table 6) of photometry and spectroscopy. The upper panels show the observations (dots) of the primary (left panel) and the secondary (right panel) and their respective fits.

gets a color excess $E(b-y) = 0\overset{\mathrm{m}}{.}154 \pm 0\overset{\mathrm{m}}{.}01$, and thereby $(b-y)_0 = -0\overset{\mathrm{m}}{.}071$, $(u-b)_0 = 0\overset{\mathrm{m}}{.}45$, $c_0 = 0.38$, $m_0 = 0.106$. From the color excess, we estimate the total visual absorption $A_\mathrm{V} \simeq 4.3\,E(b-y) = 0\overset{\mathrm{m}}{.}66$. This gives the combined visual magnitude corrected for interstellar extinction as $V_0 = 8\overset{\mathrm{m}}{.}14$, and for the mean component we get $V_0 = 8\overset{\mathrm{m}}{.}89$. From Moon's (1984) empirical calibration of the intrinsic color index $(b-y)_0$ in terms of the visual surface brightness parameter F_V, defined as $F_\mathrm{V} = 4.2207 - 0.1\,V_0 - 0.5\,\log\Phi_\mathrm{ld}$ (Barnes & Evans 1976), we then derive $F_\mathrm{V} = 4.080 \pm 0.03$ and $\Phi_\mathrm{ld} = 0''032 \pm 0''001$.

Various temperature calibrations with Strömgren indices lead to closely concordant results summarized in KK. E.g., the (c_0, T_eff)-calibration of Davis & Shobbrook (1977) for luminosity class V-III, in conjunction with Code et al.'s (1976) (T_eff, $B.C.$)-relation gives $T_\mathrm{eff} \simeq 16000 \pm 500$ K, $B.C. \simeq -1.52 \pm 0.10$. From interpolation in the theoretical grids of Lester et al.

Table 3. Parameters derived from the radial velocities and the light curves with the Levenberg-Marquard algorithm. Units are as in Table 2. In addition, $M1$ and $M2$ denote masses in solar mass units, $R1$ and $R2$ denote the radii in solar radius units, $T2$ is the temperature in units of 10,000 Kelvin, and L_{1U}, L_{1B} and L_{1V} are the luminosities as defined in the WD program, Ω_1 and Ω_2 denote the Roche potentials, f_1 and f_2 the filling factors indicating that BF Aur is detached. The parameters ℓ_U, ℓ_B and ℓ_V are the ratios of L_2/L_1 in the specific passbands. The parameter, r, in the last column of this table is defined as the maximum of all ratio "parameter correction over standard deviation".

q	$\sigma_{\rm fit}$	M1	M2	R1	R2	a	γ	i	T_2	Ω_1	Ω_2	L_{1U}	L_{1B}	L_{1V}	ℓ_U	ℓ_B	ℓ_V	$-f_1$	$-f_2$	r
0.800	4.615	5.05	4.04	4.36	4.23	11.914	0.360	84.520	1.559	3.624	3.444	6.320	6.317	6.305	0.914	0.919	0.923	-0.460	-0.059	1.264
0.810	4.609	5.05	4.09	4.37	4.25	11.939	0.359	84.503	1.558	3.636	3.464	6.313	6.309	6.297	0.917	0.922	0.926	-0.443	-0.066	0.030
0.820	4.604	5.05	4.14	4.38	4.26	11.962	0.357	84.506	1.556	3.641	3.488	6.338	6.333	6.320	0.910	0.914	0.919	-0.413	-0.081	1.601
0.830	4.604	5.06	4.20	4.37	4.28	11.990	0.356	84.440	1.557	3.664	3.503	6.277	6.273	6.261	0.928	0.933	0.937	-0.421	-0.075	0.282
0.840	4.595	5.05	4.25	4.40	4.28	12.009	0.355	84.468	1.555	3.664	3.530	6.327	6.321	6.307	0.913	0.918	0.924	-0.382	-0.095	0.513
0.850	4.601	5.07	4.31	4.32	4.35	12.045	0.353	84.438	1.562	3.726	3.525	6.086	6.085	6.075	0.987	0.992	0.996	-0.472	-0.049	0.540
0.860	4.594	5.07	4.36	4.33	4.36	12.066	0.352	84.430	1.561	3.735	3.546	6.089	6.087	6.077	0.987	0.991	0.995	-0.452	-0.057	0.099
0.870	4.588	5.07	4.41	4.35	4.37	12.085	0.351	84.428	1.560	3.741	3.569	6.107	6.105	6.093	0.981	0.986	0.990	-0.426	-0.069	0.405
0.880	4.584	5.07	4.46	4.35	4.38	12.105	0.349	84.423	1.559	3.754	3.589	6.102	6.099	6.087	0.983	0.988	0.992	-0.412	-0.076	0.125
0.890	4.583	5.06	4.51	4.35	4.40	12.124	0.348	84.419	1.558	3.768	3.608	6.085	6.081	6.068	0.989	0.994	0.998	-0.405	-0.080	0.083
0.900	4.577	5.06	4.56	4.34	4.42	12.145	0.347	84.407	1.559	3.791	3.622	6.027	6.023	6.011	1.008	1.013	1.017	-0.414	-0.073	0.389
0.910	4.577	5.05	4.60	4.37	4.42	12.159	0.345	84.410	1.556	3.788	3.651	6.095	6.089	6.075	0.986	0.991	0.997	-0.369	-0.098	0.642
0.920	4.568	5.05	4.65	4.35	4.44	12.178	0.344	84.392	1.557	3.811	3.664	6.032	6.027	6.014	1.006	1.012	1.017	-0.379	-0.089	0.926
0.930	4.571	5.05	4.69	4.33	4.47	12.196	0.343	84.397	1.559	3.840	3.675	5.946	5.943	5.931	1.035	1.040	1.045	-0.400	-0.078	0.553
0.940	4.567	5.04	4.74	4.33	4.48	12.211	0.341	84.395	1.558	3.850	3.696	5.946	5.942	5.930	1.035	1.040	1.045	-0.385	-0.085	0.137
0.950	4.562	5.03	4.78	4.32	4.50	12.226	0.340	84.437	1.560	3.874	3.710	5.888	5.885	5.873	1.055	1.060	1.065	-0.394	-0.080	1.523
0.960	4.562	5.02	4.82	4.34	4.50	12.238	0.339	84.401	1.557	3.874	3.736	5.935	5.930	5.917	1.039	1.045	1.050	-0.360	-0.098	1.348
0.970	4.557	5.01	4.86	4.33	4.52	12.251	0.338	84.434	1.558	3.893	3.752	5.894	5.890	5.878	1.053	1.059	1.064	-0.363	-0.096	0.419
0.980	4.556	5.00	4.90	4.34	4.52	12.263	0.336	84.434	1.557	3.903	3.774	5.901	5.896	5.883	1.051	1.057	1.062	-0.347	-0.105	0.040
0.990	4.566	5.00	4.95	4.27	4.58	12.282	0.335	84.498	1.562	3.957	3.770	5.709	5.707	5.696	1.120	1.124	1.129	-0.414	-0.067	0.074
1.000	4.562	4.99	4.99	4.27	4.59	12.292	0.334	84.500	1.561	3.968	3.790	5.706	5.704	5.693	1.121	1.126	1.130	-0.401	-0.073	0.536
1.010	4.559	4.97	5.02	4.28	4.59	12.301	0.333	84.497	1.560	3.977	3.811	5.713	5.710	5.699	1.118	1.123	1.128	-0.383	-0.081	0.605
1.020	4.556	4.96	5.06	4.29	4.60	12.310	0.331	84.479	1.558	3.981	3.834	5.739	5.735	5.723	1.109	1.115	1.120	-0.358	-0.093	0.078
1.030	4.554	4.95	5.09	4.29	4.61	12.319	0.330	84.493	1.558	3.996	3.852	5.721	5.716	5.704	1.116	1.121	1.127	-0.352	-0.096	0.151
1.040	4.553	4.93	5.13	4.28	4.62	12.328	0.329	84.510	1.558	4.011	3.870	5.699	5.694	5.682	1.124	1.130	1.135	-0.348	-0.097	0.418
1.050	4.550	4.92	5.16	4.29	4.62	12.335	0.328	84.510	1.557	4.021	3.891	5.704	5.699	5.686	1.122	1.128	1.134	-0.333	-0.105	0.410
1.060	4.551	4.90	5.19	4.29	4.63	12.341	0.327	84.518	1.556	4.033	3.910	5.699	5.693	5.680	1.124	1.130	1.136	-0.322	-0.110	0.208
1.070	4.550	4.89	5.23	4.27	4.65	12.349	0.325	84.575	1.558	4.060	3.920	5.623	5.619	5.606	1.153	1.159	1.164	-0.339	-0.099	1.555
1.080	4.550	4.87	5.26	4.28	4.65	12.355	0.325	84.550	1.556	4.063	3.946	5.662	5.656	5.642	1.138	1.145	1.151	-0.313	-0.114	0.816
1.090	4.555	4.85	5.29	4.30	4.64	12.360	0.323	84.502	1.553	4.059	3.976	5.726	5.719	5.703	1.114	1.121	1.128	-0.278	-0.138	1.024
1.100	4.551	4.84	5.32	4.29	4.65	12.366	0.322	84.541	1.554	4.080	3.989	5.679	5.672	5.657	1.132	1.139	1.145	-0.284	-0.132	0.480
1.110	4.553	4.82	5.35	4.29	4.66	12.370	0.321	84.559	1.554	4.093	4.008	5.666	5.659	5.644	1.137	1.144	1.150	-0.277	-0.135	0.687
1.120	4.555	4.80	5.38	4.29	4.66	12.374	0.320	84.551	1.553	4.103	4.030	5.674	5.666	5.650	1.134	1.141	1.148	-0.265	-0.144	0.440
1.130	4.561	4.78	5.40	4.32	4.64	12.378	0.319	84.491	1.549	4.097	4.065	5.760	5.750	5.732	1.102	1.110	1.117	-0.227	-0.175	0.304
1.140	4.560	4.76	5.43	4.30	4.67	12.381	0.318	84.548	1.551	4.122	4.073	5.687	5.678	5.661	1.129	1.137	1.144	-0.240	-0.161	1.281
1.150	4.563	4.74	5.46	4.29	4.67	12.384	0.317	84.568	1.550	4.135	4.094	5.686	5.676	5.659	1.130	1.138	1.145	-0.233	-0.168	2.156
1.160	4.567	4.72	5.48	4.30	4.66	12.386	0.316	84.544	1.548	4.140	4.121	5.716	5.705	5.686	1.119	1.127	1.134	-0.215	-0.184	0.085
1.170	4.569	4.71	5.51	4.31	4.66	12.388	0.315	84.524	1.547	4.145	4.147	5.745	5.732	5.713	1.108	1.117	1.124	-0.197	-0.199	1.904
1.180	4.571	4.69	5.53	4.31	4.66	12.390	0.314	84.537	1.547	4.160	4.165	5.728	5.716	5.697	1.114	1.123	1.131	-0.193	-0.201	0.339
1.190	4.574	4.67	5.55	4.31	4.67	12.392	0.313	84.541	1.546	4.172	4.184	5.723	5.710	5.691	1.116	1.125	1.133	-0.187	-0.207	1.460
1.200	4.579	4.65	5.57	4.31	4.66	12.392	0.312	84.539	1.544	4.179	4.211	5.751	5.737	5.716	1.106	1.115	1.123	-0.172	-0.222	0.310

(1986) we get $T_{\rm eff} \simeq 15900 \pm 500$ K and $\log g \simeq 3.92 \pm 0.15$. Finally, a photometric spectral type may be derived from the position in the $[m_1] - [c_1]$ plane, which is that of an evolved B4–5V star.

5. The physical state of BF Aurigae

A change in period $\mathrm{d}P/\mathrm{d}E = 2 \cdot 1.77 \cdot 10^{-10} E^2$ days/cycle has been determined by a parabolic fit of the BF Aur O-C curve obtained by Demircan et al. (1997) which leads to the ephemeris

$$\mathrm{Min.I} = (T_0 + \Delta T_0) + (P_0 + \Delta P_0) \cdot E + \Delta P \cdot E^2$$

with $T_0 + \Delta T_0 = 2449002.0253$, $P + \Delta P = 1.5832219$ and $\Delta P = 1.77 \cdot 10^{-10}$, and the integer-valued quantity E denoting the epoch (number of cycles measured from T_0). The period increase measured in days/cycle is equivalent to a weak period increase of $\mathrm{d}P/\mathrm{d}t = 0.0071\mathrm{s/yr}$. which is of the same order as the value $\mathrm{d}P/\mathrm{d}t = 0.00658\mathrm{s/yr}$ obtained by Zhang et al. (1993) or the value $\mathrm{d}P/\mathrm{d}t = 0.0070\mathrm{s/yr}$ found by Simon (1999). Note however, that Fig. 8 in KK shows that the period has remained practically constant over more than 70 years of observational records.

Although the accuracy of the data is quite high, q is only weakly defined and at present the question whether q is larger or

Table 4. Parameters derived from the radial velocities and the light curves with the Levenberg-Marquard algorithm under the additional constraint that the secondary fills its Roche lobe. Ω_1 and Ω_2 denote the Roche potentials; the filling factors $f_1 < 0$ and $f_2 = 0$ indicate that BF Aur is semi-detached with the secondary component filling its Roche lobe. Otherwise as in Table 3.

q	$\sigma_{\rm fit}$	M1	M2	R1	R2	a	γ	i	T_2	Ω_1	L_{1U}	L_{1B}	L_{1V}	f_1	f_2	r
0.800	4.691	5.08	4.06	4.26	4.30	11.939	0.360	84.441	1.568	3.687	6.040	6.042	6.035	-0.599	0.000	0.004
0.810	4.690	5.08	4.12	4.26	4.33	11.967	0.358	84.435	1.567	3.706	6.003	6.005	5.998	-0.598	0.000	0.035
0.820	4.694	5.09	4.17	4.25	4.35	11.993	0.357	84.451	1.567	3.729	5.958	5.960	5.953	-0.604	0.000	0.021
0.830	4.694	5.09	4.23	4.25	4.37	12.019	0.355	84.430	1.567	3.746	5.926	5.927	5.920	-0.598	0.000	0.000
0.840	4.701	5.10	4.28	4.24	4.39	12.043	0.354	84.430	1.568	3.766	5.883	5.885	5.879	-0.599	0.000	0.314
0.850	4.692	5.10	4.33	4.23	4.41	12.066	0.353	84.430	1.568	3.784	5.847	5.849	5.843	-0.595	0.000	0.176
0.860	4.693	5.10	4.39	4.22	4.43	12.087	0.351	84.484	1.569	3.808	5.795	5.798	5.792	-0.604	0.000	0.108
0.870	4.682	5.10	4.43	4.22	4.45	12.107	0.350	84.503	1.570	3.823	5.766	5.769	5.763	-0.595	0.000	0.454
0.880	4.684	5.10	4.48	4.21	4.47	12.128	0.348	84.515	1.569	3.843	5.733	5.736	5.730	-0.595	0.000	0.167
0.890	4.684	5.09	4.53	4.21	4.49	12.148	0.347	84.507	1.569	3.860	5.702	5.704	5.698	-0.590	0.000	0.041
0.900	4.690	5.09	4.58	4.21	4.51	12.168	0.346	84.505	1.569	3.877	5.672	5.674	5.668	-0.586	0.000	0.060
0.910	4.691	5.09	4.63	4.20	4.53	12.185	0.345	84.536	1.569	3.899	5.631	5.633	5.627	-0.590	0.000	0.000
0.920	4.693	5.08	4.67	4.19	4.55	12.202	0.343	84.556	1.569	3.917	5.596	5.599	5.593	-0.589	0.000	0.047
0.930	4.692	5.07	4.72	4.18	4.56	12.217	0.342	84.580	1.569	3.935	5.566	5.568	5.562	-0.586	0.000	0.571
0.940	4.694	5.07	4.76	4.17	4.58	12.232	0.341	84.628	1.570	3.956	5.526	5.528	5.522	-0.590	0.000	0.052
0.950	4.695	5.06	4.80	4.17	4.60	12.246	0.339	84.635	1.570	3.970	5.502	5.504	5.499	-0.580	0.000	0.561
0.960	4.710	5.05	4.85	4.16	4.61	12.259	0.338	84.699	1.571	3.993	5.456	5.459	5.454	-0.587	0.000	0.383
0.970	4.702	5.04	4.89	4.14	4.63	12.271	0.337	84.772	1.572	4.015	5.414	5.418	5.413	-0.592	0.000	0.207
0.980	4.697	5.03	4.93	4.13	4.64	12.283	0.336	84.833	1.572	4.036	5.378	5.381	5.377	-0.596	0.000	0.197
0.990	4.695	5.01	4.96	4.13	4.66	12.294	0.334	84.836	1.572	4.051	5.354	5.358	5.353	-0.589	0.000	0.010
1.000	4.699	5.00	5.00	4.12	4.67	12.304	0.333	84.852	1.572	4.067	5.330	5.333	5.329	-0.583	0.000	0.025
1.010	4.704	4.99	5.04	4.11	4.69	12.314	0.332	84.906	1.572	4.089	5.293	5.296	5.291	-0.587	0.000	0.242
1.020	4.708	4.97	5.07	4.11	4.70	12.322	0.331	84.936	1.571	4.104	5.270	5.272	5.268	-0.580	0.000	0.169
1.030	4.709	4.96	5.11	4.09	4.72	12.331	0.329	85.005	1.572	4.127	5.231	5.234	5.229	-0.585	0.000	0.572
1.040	4.714	4.94	5.14	4.09	4.73	12.338	0.328	85.009	1.572	4.138	5.216	5.219	5.214	-0.572	0.000	0.028
1.050	4.722	4.93	5.17	4.08	4.74	12.345	0.327	85.085	1.572	4.160	5.178	5.181	5.176	-0.577	0.000	0.002
1.060	4.718	4.91	5.21	4.07	4.76	12.351	0.326	85.160	1.572	4.181	5.143	5.146	5.141	-0.580	0.000	0.958
1.070	4.725	4.90	5.24	4.07	4.77	12.357	0.325	85.174	1.572	4.194	5.128	5.130	5.125	-0.569	0.000	0.253
1.080	4.736	4.88	5.27	4.06	4.78	12.362	0.323	85.218	1.572	4.210	5.103	5.106	5.101	-0.564	0.000	0.149
1.090	4.746	4.86	5.30	4.04	4.79	12.365	0.322	85.340	1.572	4.235	5.059	5.062	5.057	-0.575	0.000	0.402
1.100	4.751	4.84	5.32	4.03	4.80	12.368	0.321	85.409	1.572	4.254	5.030	5.033	5.028	-0.575	0.000	0.148
1.110	4.760	4.82	5.35	4.01	4.81	12.370	0.320	85.537	1.572	4.277	4.991	4.994	4.989	-0.583	0.000	0.019
1.120	4.762	4.80	5.37	4.01	4.82	12.373	0.319	85.563	1.573	4.290	4.975	4.978	4.973	-0.573	0.000	0.103
1.130	4.773	4.78	5.40	4.00	4.83	12.374	0.318	85.637	1.573	4.307	4.949	4.952	4.947	-0.571	0.000	0.157
1.140	4.781	4.76	5.42	3.99	4.84	12.375	0.317	85.744	1.573	4.327	4.917	4.920	4.915	-0.573	0.000	0.196
1.150	4.794	4.73	5.44	3.98	4.85	12.375	0.315	85.818	1.573	4.343	4.895	4.898	4.894	-0.569	0.000	0.576
1.160	4.802	4.71	5.47	3.97	4.86	12.376	0.314	85.898	1.573	4.359	4.873	4.875	4.871	-0.567	0.000	0.059
1.170	4.820	4.69	5.49	3.96	4.87	12.374	0.313	86.002	1.573	4.377	4.846	4.849	4.844	-0.566	0.000	0.017
1.180	4.837	4.67	5.51	3.96	4.88	12.374	0.312	86.034	1.573	4.389	4.833	4.836	4.832	-0.556	0.000	0.160
1.190	4.858	4.64	5.53	3.95	4.89	12.371	0.311	86.155	1.573	4.407	4.806	4.809	4.805	-0.556	0.000	0.183
1.200	4.885	4.62	5.54	3.94	4.90	12.369	0.310	86.224	1.574	4.422	4.788	4.791	4.787	-0.551	0.000	0.006

smaller than unity cannot be decided with certainty. So, the best we can do is discuss the possible scenarios and their implications on the astrophysical state of BF Aur.

Scenario 1: The observed period change has the right sign for mass reversal if we get a solution with $q < 1$, $k > 1$ and $\ell_2/\ell_1 > 1$ (implied by the stronger lines of the photometric secondary which is the spectroscopic primary and in agreement with the least squares results). The lower mass star fills or almost fills its Roche lobe. In that case we have conservative mass exchange (the system loses no mass), and mass reversal has just taken place. The period increases of BF Aur can be explained by the possible mass transfer from the less massive component to the more massive one as the case assumed in the most of Algol systems.

Scenario 2: Here we have $q \approx 1$, $k > 1$ and $\ell_2/\ell_1 > 1$. Note that Schneider et al. (1979) used the WD code in mode 5 and got a semi-detached configuration with $q \approx 1$. They point out that one should then expect BF Aur to be in the rapid phase of mass transfer from the more to the less massive component (proceeding on a thermal time scale) and thus to see a corresponding period decrease. This, however, is not observed; the period has remained practically constant over more than 70 years of ob-

Table 5. Parameters derived from the radial velocities and the light curves with the Levenberg-Marquart algorithm and free mass ratio. Ω_1 and Ω_2 denote the Roche potentials, f_1 and f_2 the filling factors indicating that BF Aur is detached. The second line specifies the standard deviations of the estimated parameters. The solution in this table is referred to as *solution 1*.

q	$\sigma_{\rm fit}$	M1	M2	R1	R2	a	γ	i	T_2	Ω_1	Ω_2	L_{1U}	L_{1B}	L_{1V}	f_1	f_2	r
0.961	4.562	5.02	4.83	4.33	4.51	12.240	0.339	84.440	1.559	3.884	3.733	5.893	5.889	5.878	-0.329	-0.120	0.549
0.004	–	0.35	0.37	0.10	0.11	0.293	0.035	0.061	0.003	0.013	0.012	0.060	0.058	0.057	–	–	–

Table 6. Parameters derived from the radial velocities and the light curves with the Levenberg-Marquart algorithm and free mass ratio. Ω_1 and Ω_2 denote the Roche potentials, f_1 and f_2 the filling factors indicating that BF Aur is detached. The second line specifies the standard deviations of the eastimated parameters. The solution in this table is referred to as *solution 2*.

q	$\sigma_{\rm fit}$	M1	M2	R1	R2	a	γ	i	T_2	Ω_1	Ω_2	L_{1U}	L_{1B}	L_{1V}	f_1	f_2	r
1.048	4.550	4.92	5.16	4.29	4.62	12.334	0.328	84.517	1.557	4.020	3.886	5.697	5.692	5.679	-0.462	-0.058	0.313
0.005	–	0.35	0.37	0.10	0.11	0.295	0.035	0.053	0.002	0.012	0.013	0.052	0.051	0.049	–	–	–

Table 7. Full parameter set describing the adopted light curve solution for BF Aur, together with estimated uncertaintities of the main parameters. $\Delta T = (T_1 - T_2)/T_1$ measures the relative difference of the mean effective temperatures, J is the surface brightness. F_1 and F_2 denote the fill-out parameter Ω_c/Ω. S and V denote surface area and volume. k is the ratio of the mean radii.

$q = 1.048 \pm 0.008$	$\Omega_c = 3.828$	$\Omega_1 = 4.0205$	$\Omega_2 = 3.8857$
$r_{1pole} = 0.3305$	$r_{2pole} = 0.3532$	$F_1 = 95.2\%$	$F_2 = 98.5\%$
$r_{1point} = 0.3921$	$r_{2point} = 0.4473$	$S_1 = 1.596$	$S_2 = 1.697$
$r_{1side} = 0.3438$	$r_{2side} = 0.3700$	$V_1 = 0.189$	$V_2 = 0.206$
$r_{1back} = 0.3659$	$r_{2back} = 0.3978$	$R_1 = 4.29 \pm 0.10$	$R_2 = 4.62 \pm 0.11$
$i = 84.8 \pm 0.06$		$k = 1.08 \pm 0.04$	
$(L_2/L_1)_U = 1.124$	$(J_2/J_1)_{pole} = 0.987$	$(J_2/J_1)_U$ = 1.166	
$(L_2/L_1)_B = 1.134$	$(J_2/J_1)_{pole} = 0.990$	$(J_2/J_1)_B$ = 1.166	
$(L_2/L_1)_V = 1.136$	$(J_2/J_1)_{pole} = 0.990$	$(J_2/J_1)_V$ = 1.166	
$M_{1bol} = -2.74$	$M_{2bol} = -2.84$	$\Delta M = 0.10$	$\Delta T = 0.014$

servational records (see Fig. 8 in KK), and the newer results even indicate a period increase. The likely reason for this is that the period change due to mass transfer is proportional to $|q-1|$, which probably is much smaller than thought before. It may be estimated that, if only 5–10% of the material lost by the primary is lost from the system (non-conservative case), a period decrease might be compensated or even turned into a period increase (see the discussion in by Wilson and Stothers (1995) related to the non-conversation of angular momentum, or transformation of orbital angular momentum into rotational angular momentum). Note that there is no problem being in the rapid phase past mass reversal. One should not assume that the rapid phase should stop when the masses equalize. Conservative mass transfer theory predicts that the rapid phase will continue far beyond the equal-mass point. For example, U Cep is widely believed to be in the rapid phase (or just coming to the end of it) although the mass donor is considerably less massive than the acceptor.

Scenario 3: We have $q > 1$, $k > 1$ and $\ell_2/\ell_1 > 1$; our light curve analysis suggests that BF Aur is still barely underfilling its Roche lobe so that mass transfer has not yet fully developed. The more massive star almost fills its Roche lobe. Since q is just above unity all arguments of scenario 2 apply as well. Let us now compare our results with respect to the mass-luminosity relation which we expect to be fulfilled for main-sequence components of close binary systems as long as mass transfer has not yet influenced their evolution. Taking $L \approx \mathcal{M}^4$, we should have $\Delta M_{\rm bol} \simeq 10\ \log q \simeq 0\overset{\rm m}{.}8 \pm 0\overset{\rm m}{.}2$. A solution compatible with the mass-luminosity relation should fulfill $q \simeq \sqrt{R_2/R_1}$ for equal temperatures. Since the ratio of radii is about 1.08 ± 0.04 for all reasonable solutions, this indicates a mass ratio near 1.04. Fig. 5 in KK shows that the bolometric magnitude difference between the binary components, as predicted from the light curve solutions, is a flat function of q (which means that the observed spectral line ratios can only be used to solve the transit/occultation question but not to discriminate between mass ratios) while the mass-luminosity relation is a steep function of q. The intersection occurs at $q \cong 1.06$ which corresponds well to the solution $q = 1.048$ in Table 3.

Table 8. This table shows the ratio $\ell_{2B}(\theta)/\ell_{1B}(\theta)$ as a function of phase θ and the mass ratio q; these values were computed with Wilson's subroutine LC. The mass ratio $q = 0.961$ ($q = 1.048$) corresponds to the solution in Table 5 (6).

$q \backslash \theta$	0.25	0.70	0.75
0.961	1.118	1.134	1.118
1.048	1.145	1.158	1.145

Table 9. Strömgren indices of BF Aur taken from the survey of Hilditch & Hill (1975). Reddening-free (bracketed) indices were computed as $[c_1] = c_1 - 0.20(b-y)$, $[m_1] = m_1 + 0.32(b-y)$, $[u-b] = (u-b) - 1.56(b-y)$.

Phase	$(b-y)$	c_1	m_1	$[c_1]$	$[m_1]$	$[u-b]$	V
0.8311[1]	0.092[1]	0.386[1]	0.030[1]	0.368[1]	0.059[1]	0.486[1]	8.79
0.0896	0.079	0.414	0.055	0.398	0.080	0.559	8.98[1]
0.1639	0.077	0.388	0.067	0.373	0.092	0.556	8.81
0.3492	0.091	0.434	0.046	0.416	0.075	0.566	8.80
0.4318	0.084	0.398	0.058	0.381	0.085	0.551	8.99[1]
mean	0.083	0.409	0.057	0.392	0.083	0.558	8.80
stdev	0.006	0.020	0.009	0.019	0.007	0.006	0.01

[1] Measurements discarded from mean values.

Table 10. Astrophysical data for BF Aur. H is the orbital angular momentum in units of 10^{52} g cm^{2}s^{-1}; h is the angular momentum per unit of reduced mass in units of 10^{18} cm^2 s^{-1}; $J_c = q(1+q)^{-2}p^{1/3} \approx H/\mathcal{M}^{5/3}$ is the specific angular momentum, and $<\rho>$ is the mean stellar density in g cm^{-3}. We define as primary the component eclipsed at primary minimum (phase $0\overset{p}{.}0$), which has, however, lower mass and luminosity, i.e., it is the spectroscopic secondary.

Parameter	Primary	System	Secondary
P (days)		1.58322	
q		1.048 ± 0.005	
H		16.3 ± 0.5	
h		33.3 ± 1.3	
$\log J_c$		-0.536 ± 0.02	
$\mathcal{M}/\mathcal{M}_\odot$	4.92 ± 0.35		5.16 ± 0.37
$\mathcal{R}/\mathcal{R}_\odot$	4.29 ± 0.10		4.62 ± 0.11
$<\rho>$	0.087 ± 0.02		0.073 ± 0.02
$\log g$ (cgs)	3.87 ± 0.03		3.82 ± 0.03
$T_{\rm eff}$ (K)	15800 ± 200		15570 ± 200
$\log \mathcal{L}/\mathcal{L}_\odot$	3.26 ± 0.1		3.30 ± 0.1
$M_{\rm bol}$	-2.74 ± 0.1		-2.84 ± 0.1
$B.C.$	-1.5		-1.5
$M_{\rm V}$	-1.3 ± 0.1		-1.5 ± 0.1
$E(b-y)$		0.154 ± 0.01	
$A_{\rm V}$		0.66 ± 0.01	
V_0		8.14 ± 0.01	
$(m-M)$		10.3 ± 0.15	
Dist. (pc)		1150 ± 80	

6. Discussion

Due to a more reliable photometric analysis and a more realistic physical model (which considers, for instance, proximity effects in the computation of the radial velocity curves and the Kurucz stellar atmospheres) the discrepancy between a pure photometric mass ratio and the spectroscopic mass ratio of unity derived by Mammano et al. (1974) from their spectrographic orbit, has been alleviated considerably. The remaining difference is in magnitude and in the sense what we have to expect considering possible systematic error sources.

Despite the remaining uncertainties of the current simultaneous analysis of spectroscopic and photometric data, we adopt the following values for further discussion: $q = 1.048$ and $a = (12.33 \pm 0.295)R_\odot$ from which we derive $\mathcal{M}_1 \simeq (4.92 \pm 0.35)\mathcal{M}_\odot$, $\mathcal{M}_2 \simeq (5.16 \pm 0.37)\mathcal{M}_\odot$, and a mean $\log g$ of 3.87 ± 0.04 consistent with the value estimated from the Strömgren indices. Together with $\log \bar{\mathcal{M}} = 0.74 \pm 0.10$ and $\log \bar{T}_{\rm eff} = 4.205 \pm 0.015$, this corresponds to a quite evolved stage on the main sequence. Further astrophysical parameters derived for the BF-Aur system are given in Table 10. The least squares solution clearly shows that the fits of the detached solutions are better than the fits of the semi-detached solutions.

The period change detected by Demircan et al. (1997) may be interpreted as an indication for mass transfer. It seems that the phase of rapid mass transfer is about to start in BF Aur. This interpretation is consistent with the classification of BF Aur by Plavec (1968): the more massive component nearly fills its Roche lobe during its slow expansion (in phase I), or the systems actually is in the process of mass exchange.

7. Conclusions

Despite the availability of consistent and more accurate photometric light curves and radial velocity curves of both components, BF Aurigae remains a difficult system for determining the mass ratio. Fits of similar quality are achieved for $0.9 \leq q \leq 1.06$ with a slight preference derived from the line ratios for $q = 1.048$ yielding $\mathcal{M}_1 = 4.92\mathcal{M}_\odot$ and $M_2 = 5.16\mathcal{M}_\odot$. The absolute masses are confined to the intervals $[4.80, 5.04]$ and $[4.20, 5.40]$.

BF Aur is best understood as a pair of evolved stars of spectral type B5V, of which the more massive component (the spectroscopic primary or photometric secondary, respectively) now almost fills its Roche lobe. Although BF Aur may be on the verge of becoming an inverse Algol (the configuration suggested by Schneider et al. 1979), interactions are of small scale and Roche lobe overflow probably has not yet fully developed.

Acknowledgements. KGS is very grateful to the Austrian Fond zur Förderung der wissenschaftlichen Forschung for support under grants S7302-AST (Doppler imaging) and S7301-AST (APT). We thank M. Weber (IfA, Vienna), for measuring the radial velocities. It is a pleasure to thank Dr. R. E. Wilson (University of Florida) for providing explanations on his light curve program, and his comments on this analysis.

Appendix A: numerical data

The tables in the Appendix are available only in electronic form at CDS, Strasbourg and list the entire APT photometry versus heliocentric Julian date (HJD). Note, that each filter magnitude is given in a separate table because the HJDs are slightly different for each measurement. The $U-B$ and $B-V$ colors are listed as well.

References

Barnes T.G., Evans D.S., 1976, MNRAS 174, 489
Breinhorst R.A., Kallrath J., Kämper B.-C., 1989, MNRAS 241, 559

Code A.D., Davis J., Bless R.C., Hanbury Brown R., 1976, ApJ 203, 417
Crawford D.L., 1978, AJ 83, 48
Davis J., Shobbrook R.R., 1977, MNRAS 178, 651
Demircan O., Özdemir S., Albayrak B., et al., 1997, Rev. Mex. Astron. Astrofis. 33, 131
Hilditch R.W., Hill G., 1975, MNRAS 79, 101
Kallrath J., Kämper B.C., 1992, A&A 265, 613 (KK)
Kallrath J., Milone E.F., 1999, Eclipsing Binaries – Modeling and Analysis, New York: Springer
Kallrath J., Milone E.F., Terrell D., Young A.T., 1998, ApJS 508, 308
Kaluzny J., Semeniuk I., 1984, Acta Astron. 34, 433
Kurucz R.L., 1979, ApJS 40, 1
Lester J.B., Gray R.O., Kurucz R.L., 1986, ApJS 61, 509
♣ Lichtenknecker D., 1989, priv. commun.
Linnell A.P., Proctor D.D., 1970, ApJ 162, 683
Mammano A. M., Margoni R., Stagni R., 1974, A&A 35, 143
Mannino G., Bartolini C., Biolchini R., 1964, Mem. Soc. Astron. Ital. 35, 371
Moon T.T., 1984, MNRAS 211, 21P
Morgenroth O., 1935, Astron. Nachr. 255, 425
Plavec M., 1968, Adv. in Astron. Astrophys. 6, 201
Popper D.M., 1980, ARA&A 18, 115
Popper D. M., 1981, ApJS 47, 339
Roman N.G., 1956, ApJ 123, 246
Schneider D.P., Darland J.J., Leung K.C., 1979, AJ 84, 236 (SDL)
Simon V., 1999, A&AS 134, 1
Strassmeier K.G., Boyd L.J., Epand D.H., Granzer Th., 1997, PASP 109, 697
Twigg L.W., Rafert J.B., 1980, MNRAS 193, 775
Van Hamme W., 1993a, AJ 106, 2096
Van Hamme W., 1993b, The new Wilson Reflection treatment and the nature of BF Aurigae. In: Milone E.F. (ed.), Light Curve Modeling of Eclipsing Binary Stars. New York: Springer, p. 53
Wilson R.E., 1979, ApJ 234, 1054
Wilson R.E., 1988, Physical models for close binaries and logical constraints. In: Leung K.-C. (ed.), Critical Observations Versus Physical Models for Close Binary Systems, Montreux, Switzerland: Gordon and Breach, p. 193
Wilson R.E., Devinney E.J., 1971, ApJ 166, 605
Wilson R.E., Stothers R., 1995, MNRAS 170, 497
Zhang R.-X., Kim J.Y.S., Zhang J.T., et al., 1993, IAU Inform. Bull. Var. Stars 3941, 1-4